doi:10.4149/neo_2014_085

Realgar (As_4S_4) nanoparticles and arsenic trioxide (As_2O_3) induced autophagy and apoptosis in human melanoma cells in vitro

M. PASTOREK[1], P. GRONESOVA[1], D. CHOLUJOVA[1], L. HUNAKOVA[1], Z. BUJNAKOVA[2], P. BALAZ[2], J. DURAJ[1], T. C. LEE[3], J. SEDLAK[1,*]

[1]Cancer Research Institute, Slovak Academy of Sciences, Bratislava, 833 91, Slovakia; [2]Institute of Geotechnics, Slovak Academy of Sciences, Kosice, 043 53, Slovakia; [3]Institute of Biomedical Sciences, Academia Sinica, Taipei, 11529, Taiwan

**Correspondence: jan.sedlak@savba.sk*

Received June 15, 2014 / Accepted July 4, 2014

The aim of the present study was to compare the effect of realgar nanoparticles and arsenic trioxide (ATO) on viability, DNA damage, proliferation, autophagy and apoptosis in the human melanoma cell lines BOWES and A375. The application of various flow cytometric methods for measurements cell viability, DNA cell cycle, mitochondrial potential, lysosomal activity, and intracellular content of glutathione was used. In addition, quantitative PCR, western blotting and multiplex bead array analyses were applied for evaluation of redox stress, autophagic flux, and cell signaling alterations.

The results showed that realgar treatment of studied cells caused modulation of cell proliferation, induced a block in G2/M phase of the cell cycle and altered phosphorylation of IκB, Akt, ERK1/2, p38, and JNK kinases, as well as decreased mitochondrial membrane potential. Additionally, it appeared that induction of cell death by both realgar and ATO was dose-dependent, when lower (0.3 μM) dosage increased lysosomal activity and induced autophagy and higher (1.25 μM) concentration resulted in the appearance of apoptosis, while pan-caspase inhibitor attenuated more efficiently realgar- than ATO-induced cell death. Furthermore, low concentrations of ATO and realgar nanoparticles increased the content of intracellular glutathione and elevated γ-H2AX expression confirmed DNA damage preferentially at higher concentrations of both drugs used. Further analysis revealed slight differences in time-dependent phosphorylation pattern due to both realgar and ATO treatments, while significant differences were noticed between cell lines.

In conclusion, realgar nanoparticles and ATO treatment induced dose-dependent activation of autophagy and apoptosis in both melanoma cell lines, when autophagy flux was determined at lower drug concentrations and the switch to apoptosis occurred at higher concentrations of both arsenic forms.

Key words: realgar, autophagy, cell cycle, DNA damage, Nrf2, chloroquine, Z-VAD-FMK, glutathione

Arsenic has been accepted to be a poison for years and it is generally considered as an extremely effective environmental co-carcinogen for some human malignancies, especially for skin and lung cancer [1]. The toxicity of arsenicals depends on their chemical states, exposure dose, the biological species, age and gender, as well as on individual susceptibilities, genetic and nutritional factors [2]. Largely, to living organisms methylated trivalent arsenicals are more toxic and pentavalent metabolites are less toxic than arsenite (iAs^{III}) [3, 4]. In 2002, a pilot clinical study of pure realgar in treatment of patients with APL was conducted in China, and impressive responses were achieved and reported [5]. Realgar is a mineral composed mainly of tetra-arsenic tetra-sulfide (As_4S_4), which is also called red arsenic due to its a deep red color (Xionghuang in Chinese). Low solubility of arsenic in realgar, using water as a solvent (0.4%), can be increased to approximately 1.5% by leaching in artificial body fluid [6]. Higher proportion of arsenic is accessible for absorption from traditional Chinese medicine formulae such as Niuhang Jiedu Pian, a Chinese over-the-counter pill containing arsenic in the form of realgar [7], where its toxicity is alleviated by four herbs present in formula and is lower than toxicity of realgar alone [8]. Several physical, chemical or biological procedures are proposed to improve the solubility of realgar [9-11]. Among them, high-energy milling belongs to one of the most promising tools for improvement of realgar solubility due to the decreasing of particle diameter to the nanosize scale [12-14].

Arsenic trioxide (ATO, As_2O_3) appeared as a small reactive molecule with high affinity for sulfhydryl groups of biomolecules like glutathione and cysteinyl residues in proteins. There

is a wide spectrum of ATO effects, such as HIF-dependent stimulation of angiogenesis, the expression of BH3-only proteins, HSP90 or 14-3-3ζ-mediated induction of apoptosis, Syk kinase-related activation of neutrophil toxicity and many others [15-18]. Although arsenic exposure leads to production of reactive oxygen species and modulates plethora signal transduction cascades [19, 20], arsenic-exposed never smokers mainly show the alterations of global histone H3 methylation, DNA copy-number in lung squamous cell carcinomas and genomic DNA methylation in urothelial carcinomas [21-23]. Daily administration of ATO in rats caused more oxidative DNA damage, higher urinary levels of 8-hydroxy-2'-deoxyguanosine than caused realgar and may be more genotoxic [24].

Because there are only a few articles directly comparing nanoparticles (NPs) of realgar with ATO, we have chosen two melanoma cell lines BOWES and A375 to determine the effect of both arsenic forms (particulate and soluble) upon the cell viability, mitochondrial membrane potential, cell cycle and DNA damage, cell signaling and cell lysosomal activity, as well as the activation of Nrf2 pathway and intracellular level of glutathione.

Our comparison of realgar and ATO effects upon the γ-H2AX histone expression, a biomarker of DNA damage, resulted in observation that similar effect of both realgar and ATO occurred preferentially at their higher concentration. Similarly, we found that there are quantitative differences between NP realgar and ATO in the course of autophagy; while the autophagic flux dominates at lower concentration and the switch to apoptosis occurs at higher concentration of both arsenic forms, NP realgar is more pro-apoptotic compound than ATO in the tested melanoma cell lines.

Material and methods

Reagents. Realgar NPs were prepared using commercial arsenic(II) sulfide (98% in purity, Sigma-Aldrich, USA) and mineral realgar collected from Allchar locality (R. Macedonia), in a laboratory circulation mill MiniCer (Netzsch, Germany) in the presence of 0.5% polyvinylpyrrolidone (PVP) and yttrium stabilized ZrO_2 milling balls [25]. JC-1 (5,5',6,6'-tetrachloro-1,1',3,3'-tetraetylbenzimidazolylcarbocyanine iodide), LysoTracker® Red DND-99 and fluorescein diacetate (FDA) were purchased from Molecular Probes (Eugene, OR, USA). Propidium iodide (PI), RNA-se A, monochlorobimane (MCB), N-Benzyloxycarbonyl-Val-Ala-Asp(O-Me) fluoromethyl ketone (Z-VAD-FMK), N-etylmaleimide (NEM), chloroquine diphosphate (CQ) and buthionine sulfoximine (BSO) were obtained from Sigma Chemical Co. (St. Louis, MO, USA). Polyclonal phospho-histone H2A.X (Ser139), LC3B (D11), and SQSTM1/p62 antibodies were obtained from Cell Signaling Technology, Inc. (MA, USA). Polyclonal antibodies against PARP-1 (A-20), β-actin (N-21), secondary HRP-IgGs and chemiluminiscence reagent (ECL) were products of Santa Cruz Biotechnology, Inc. (CA, USA).

Cells and experiment procedures. Human melanoma cell lines BOWES and A375 were routinely cultured in RPMI 1640 medium supplemented with 10% heat-inactivated FCS, 2 mM L-glutamine, 100 μg/ml penicillin and 50 μg/ml streptomycin, in 5% CO_2 humidified atmosphere, at 37 °C. For the experiments, approximately 0.5 x 10^6 cells/ml were plated in 96, 12 or 6 well plates (Greiner, Germany), cultivated for 24 h, and then treated with realgar or ATO different time periods. For inhibition of apoptosis, autophagy and GSH synthesis, pre-treatment with 10 μM Z-VAD-FMK, 10 μM CQ and 50 μM BSO, for 1 h was used.

Growth inhibition analysis. Approximately 5 x 10^3 cells/well were seeded in 96-well plates and proliferation was measured. The cells were screened by IncuCyte ZOOM (Essen BioScience, USA) for each 4 hours. Samples were prepared in quadruplicates and 0.1 % PVP was used as control for realgar treatment. Data were analyzed by IncuCyte ZOOM software.

Western blot analysis. To study changes in protein levels, cultured cells (5 x 10^6) were washed in PBS and lysed in 100 μl RIPA lysis buffer containing 1 mM PMSF and phosphatase inhibitors (2 mM sodium orthovanadate, 2 mM sodium fluoride). Eighty μg of protein lysates were run in 12.5 % SDS/PAGE gels, transferred to nitrocellulose membrane and incubated with corresponding IgGs. The protein-antibody complexes were detected using secondary HRP-IgGs followed by enhanced chemiluminescence reagent (ECL).

Phosphorylation analysis. To study cell signaling pathways, western blott lysates were used. Changes in phosphorylation of Akt (Ser473), IκB-α (Ser32/Ser36), ERK 1/2 (Thr202/Tyr204, Thr185/Tyr187), JNK (Thr183/Tyr185) and p38 MAPK (Thr180/Tyr182) kinases were measured during the interval of 1, 3, 5, and 7 hours by Bio-plex 200 (Bio-Rad, USA) using Bio-Plex® Phospho protein Assay (Bio-Rad) kit. Alterations in kinase phosphorylation were compared with the control samples.

Analysis of gene expression. BOWES and A375 cell lines were treated for 24 hours with 0.30, 0.60, and 1.25 μg/ml As in form of NP realgar and ATO. Total RNA was isolated using TRIzol® Reagent (Ambion®, USA). Two micrograms of total RNA was reverse transcribed with RevertAid™ H minus First Strand cDNA Synthesis Kit (Fermentas, Germany) using Bio-Rad C1000 Touch™ Thermal Cycler (Bio-Rad Laboratories, USA). cDNA (20x diluted) was used as a template for qRT-PCR analysis performed using Maxima SYBR Green qPCR Master Mix (2 ×) (Fermentas, Germany) and Bio-Rad CFX96™ Real-Time PCR Detection system (Bio-Rad Laboratories, USA) in 20 μl PCR reaction mix. The PCR protocol consisted of 10 min 95 °C initial denaturation, followed by 39 repeats of 30 s 95 °C denaturation, 30 s 58 °C annealing, 30 s 72 °C extension and 5 s 73 °C or 76 °C and 80°C plate reading. Gene expression analysis was calculated by Bio-Rad Software Manager, Version 1.6, provided by the manufacturer (Bio-Rad Laboratories, USA). A normalized fold expression was compared with the ΔΔCq method. The target genes nuclear factor, erythroid 2-like 2 (NRF2) NFE2L2 and heme oxygenase-1 (HO-1) HMOX1 were normalized to the reference gene β-actin from each treated sample. Analysis was performed twice in triplicates. Obtained results were analyzed by T-test.

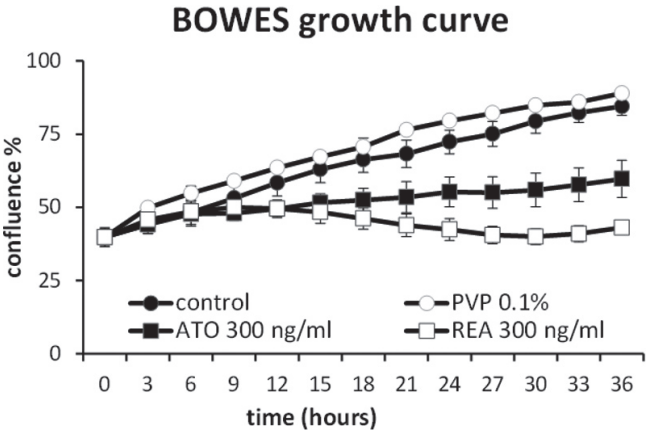

Figure 1. Effect of NP realgar and ATO treatment on BOWES cell proliferation.
BOWES cells were cultivated in the presence of NP realgar (REA) or ATO at the concentration 300 ng/ml of As for 36 hours. The effect of 0.1% PVP (detergent used for the milling of realgar) on proliferation of cells is shown. Samples were done in quadruplicates and cell confluence was screened every 3 h using IncuCyte ZOOM microscope.

The following primers were used: human β-actin:
5'-CCAACCGCGAGAAGATGACC-3' (forward)
5'-AGGATCTTCATGAGGTAGTCAGTC-3' (reverse);
human NFE2L2:
5'- AGCAGGACATGGATTTGATTG -3' (forward)
5'- TGGGAGAAATTCACCTGTCTC -3' (reverse);
human HMOX1:
5'- ATGCCCCAGGATTTGTCA -3' (forward)
5'- TGC AGCTCTTCTGGGAAGTA -3' (reverse).

Fluorescein diacetate (FDA)/PI staining. The cells were collected by centrifugation at 1000 x g for 3 min and washed twice with cold PBS. Approximately 5 x 10^5 cells were resuspended in 300 µl of PBS/0.2% BSA containing 10 nM of FDA (from a 5 mM stock in DMSO) for 30 min at room temperature. The cells were then cooled and 3 µl of PI (1 mg/ml) were added. Finally, after 15 min, the stained cells were analyzed with a Beckman FACS Canto II flow cytometer. Data was analyzed with FCS Express 4 Flow software (De Novo Software, LA, USA).

Cell cycle analysis. This assay was based on the measurement of the DNA content of nuclei labelled with propidium iodide (PI). For flow cytometry analyses of DNA cell cycle profile, approximately 5 x 10^5 cells were collected by centrifugation at 1000 x g for 3 min. The cells were washed twice with cold PBS and resuspended in 300 µl of 0.05% Triton X-100 and 15 µl of RNA-se A (10 mg/ml) in PBS for 20 min at 37 °C. Then the cells were cooled and incubated on ice for at least 10 min before PI (50 µg/ml) was added. Finally, after 15 min the stained cells were analyzed using a BD FACS Canto II flow cytometer. Data were analyzed with Multi-Cycle AV plug-in to FCS Express 3 software (De Novo Software, LA, USA).

Analysis of mitochondrial membrane potential. Cell mitochondrial membrane potential during apoptosis was measured using a JC-1 fluorescent probe. Cells with normal polarized mitochondrial membranes emit green-orange fluorescence, and the percentage of cells that emit only green fluorescence is attributable to depolarized mitochondrial membranes. Briefly, 5 x 10^5 cells were washed twice with cold PBS and incubated in 300 µl of PBS/0.2% BSA containing 4 µM of JC-1 (from a 7.7 mM stock in DMSO) at 37 °C, for 30 min in the dark, and the cells were analyzed using a BD FACS Canto II flow cytometer. Finally, data were analyzed with FCS Express 3 software.

GSH level analysis. The cells were collected by centrifugation at 1000 x g for 3 min and washed twice with cold PBS. Samples were stained for viability according to FDA/PI staining protocol and split into the two equal parts and incubated with- or without 10 mM NEM for 20 min. Both parts were then incubated with 40 µM MCB for 25 min, and after 15 min, the stained cells were analyzed with a BD FACS Canto II flow cytometer. Live cells were gated for each sample and from samples without NEM the fluorescence of NEM-treated sample was substracted to assess a net fluorescence of GSH-MCB conjugate. Data were analyzed with FCS Express 4 Flow software.

Flow cytometry measurements and data analysis. BD FACS Canto II flow cytometer was equipped with 405 nm and 488 nm excitation lasers, and fluorescence emission for different fluorochromes was measured as follows; excited with 405 nm laser: GSH-MCB (450/50) and excited with 488 nm laser: FDA (530/30), PI (585/42), JC-1 (530/30 and 585/42, ratio of 530/30 and 585/42), cell cycle (log 695/40 – sub-G1, lin 585/42 – DNA cell cycle histogram, 780/60 peak vs. integral for doublets discrimination). Forward/side light scatter characteristics were used to exclude the cell debris from the analysis. For each analysis, at least 1 x 10^4 cells were acquired.

Analysis of lysosomal activity. Following the treatments, cell culture medium was removed and replaced with medium without serum containing 60 nM LysoTracker® Red DND-99. After 1 hour of incubation, cells were collected along with dead cells from original medium and washed twice with PBS. Then the cells were stained with FDA and 3 µg/ml of 7-AAD were used instead of PI for staining of dead cells. Samples were then analyzed by ImageStreamX Mark II (Amnis, USA) at 40x magnification and data were evaluated by Inspire software 5.0 (Amnis, USA). Flourochromes were excited by 488 nm laser and flourescence emission was measured as follows: FDA (channel 1), LysoTracker® Red DND-99 (channel 4), 7-AAD (channel 5). Side scatter (darkfield) characteristics were used to exclude the cell debris from the analysis and for doublet discrimination. Changes in lysosomal activity were measured as flourescence for LysoTracker® Red DND-99 and normalized to control.

Results

Cell growth time-lapse analysis. The cytotoxic effect of NP realgar and ATO upon melanoma cell line growth was monitored using a time-lapse analysis of cell confluence during

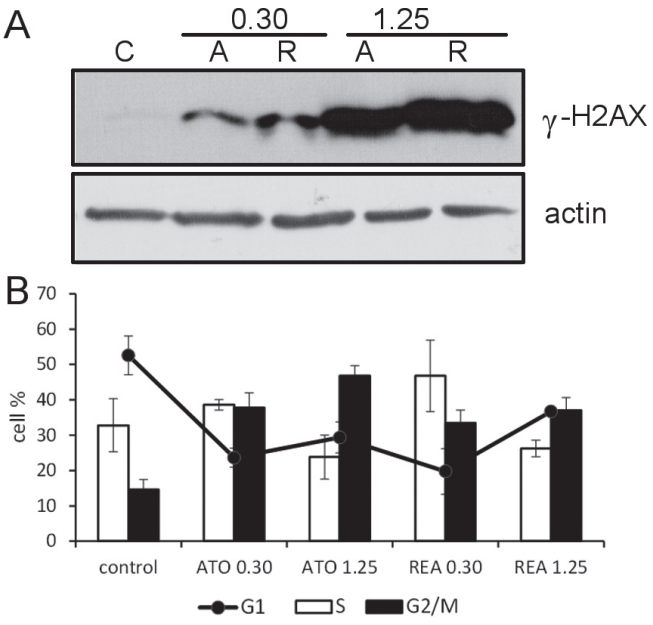

Figure 2. DNA damage and cell cycle progression of BOWES cells treated with NP realgar and ATO.
BOWES cells were treated with NP realgar (REA) and ATO at the concentration 0.30 μg/ml and 1.25 μg/ml As for 24 hours. (A) The representative western blott analysis of H2AX histone phosphorylation in control (C), REA (R), and ATO (A) treated cells is shown. (B) Flow cytometry was used to acquire data from PI-stained cells and histograms of DNA content were analyzed using Multi-Cycle AV plug-in to FCS Express 3 software. The data of three independent experiments are presented as the mean +/- standard deviation.

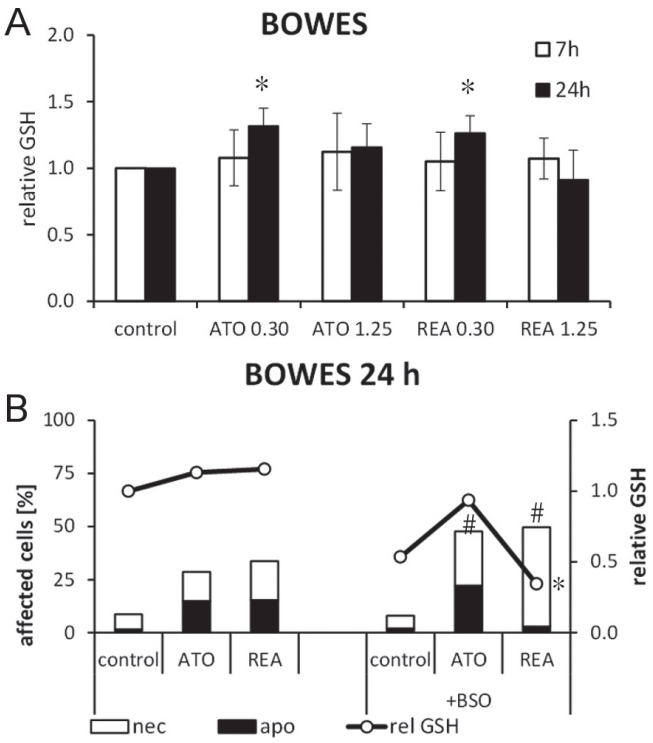

Figure 3. Changes of GSH content in BOWES cells treated with NP realgar and ATO and their modulation by BSO.
(A) BOWES cells were treated as indicated and GSH levels were measured by flow cytometry. (B) Viability data of BOWES cells affected by arsenic treatment (1.25 μg/ml As in the form of REA and ATO for 24 hours) without and with 50 μM BSO pre-treatement from three independent experiments are presented. # – significant difference ($p<0.05$) from arsenic treated cells in the absence and presence of BSO, * – statistical significance ($p<0.05$) from control cells

the 36 hours of cell treatment. The shape of growth curves confirmed the negligible cytotoxic effect of the 0.1% PVP solution used for the preparation of realgar samples, while substantial difference in the toxicity of realgar and ATO at the arsenic concentration 300 ng/ml was observed (Fig. 1). Although the growth curve of cells treated with 10 ng/ml of arsenic, corresponding to the actual upper limit of arsenic concentration in drinking water [26], superimposed the control cell curve, the growth inhibitory effect of NP realgar versus ATO was clearly visible at higher concentration of arsenic (50 ng/ml) (Fig. S1A, S1B). In addition, the sinusoidal shape of the growth curve was also preserved at higher realgar concentration (Fig. S1C).

DNA damage and G2/M cells accumulation. Because the growth rate of both cell lines treated with higher concentrations of arsenic decreased within 6 – 9 h of treatment we wanted to see the effect of NP realgar on the DNA cell cycle. We observed about 10% drop of G1 fraction at the expense of G2/M in BOWES cells (Fig. S2A), while the pattern of changes in A375 cells was more complex at 7 h of the treatment (Fig. S2B), with a faint increase of G2/M cells in ATO treated cells (Fig. S2C). Significant rise of G2/M cells was noticed in both cell lines treated for 24 h (Fig. 2B). The proportion of S phase cells also differed from the control untreated cells, suggesting the NP realgar-induced DNA damage potentially resulting from inorganic arsenic metabolism-generated reactive oxygen and nitrogen species [27]. Therefore, we analyzed phosphorylation of histone H2AX that binds to double strand breaks and serves as a sensitive marker of DNA damage. We have indeed found a clear upregulation of γ-H2AX expression in BOWES cells treated with higher concentration of realgar or ATO, whereas in A375 cells only higher concentration of realgar augmented γ-H2AX expression (Fig. 2A, S2B).

Effect of NP realgar on cellular GSH level. In cells, arsenic is bound especially to vicinal dithiols of proteins and to low molecular weight compounds such as glutathione and cysteine. Glutathione is one of the nonenzymatic, low molecular weight players maintaining intracellular redox homeostasis. In our study, increased glutathione levels were found preferentially in cells treated with lower concentrations of realgar and ATO (Fig. 3, S3A). Therefore, we have used a nontoxic concentration of BSO, a specific inhibitor of GSH synthesis, to determine whether toxicity of NP realgar depends on the amount of the intracellular GSH. Thus we have combined BSO and arsenic in the form of realgar or ATO for 24 h treatment and then the viability of cells as well as the extent of apoptosis and necrosis was measured (Fig. 3B). While there was a difference in pro-

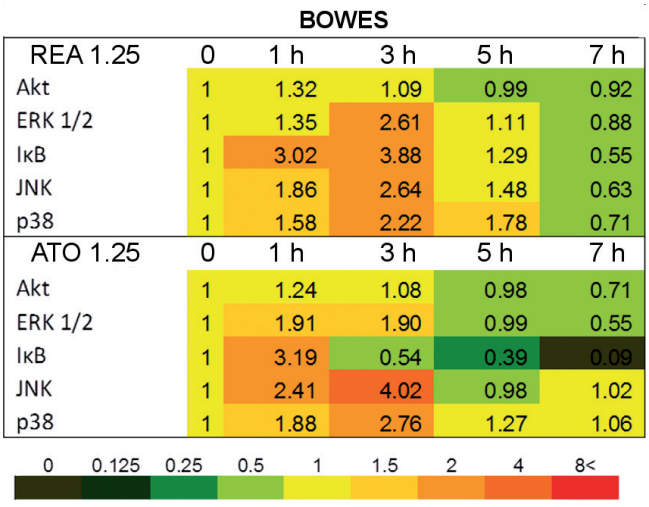

Figure 4. Modulation of Akt, ERK1/2, IκB, JNK, and p38 kinases phosphorylation by NP realgar and ATO treatment in BOWES cells.
BOWES cells were treated with 1.25 μg/ml As of NP realgar (REA) and ATO for time indicated and changes in relative phosphorylation were measured using Bio-Rad Bio-plex 200 machine. Data were normalized to the respective time-control value set to equal 1.0.

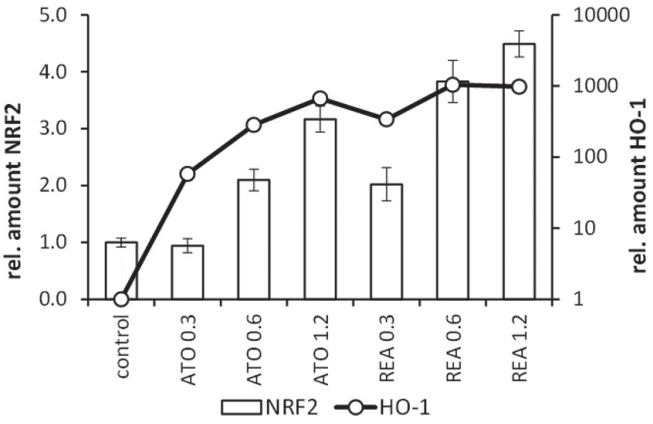

Figure 5. Quantitative PCR analysis of *NRF2* and *HO-1* mRNA expression after NP realgar and ATO treatment in BOWES cells.
BOWES cells were treated with increased concentration of As as indicated, in the form of NP realgar (REA) and ATO and expression of NRF2 and HO-1 mRNA was measured after 24 hours of treatment. The data of two independent experiments are presented.

portion of apoptotic and necrotic cells in BOWES treated cells, such difference was not observed in A375 cell line (Fig. S3B). In both cases, the toxicity of arsenic compounds was significantly increased in the presence of BSO. Analysis of FDA/PI data revealed IC_{50} values for NP realgar and ATO (0.21 and 0.43 μg/ml of As in BOWES, and 0.25 and 0.46 μg/ml of As in A375 at 72 hours, respectively; data not presented).

The NP realgar effect on phosphorylation. There are several studies showing the effect of arsenic in the form of ATO on cellular signaling, while only few ones did identify the effect of realgar. Therefore we wanted to compare time-dependent effect of NP realgar and ATO on activation of selected kinases and IκB protein that is involved in the activation of NFκB pathway. Both arsenic forms induced overall increase of phosphorylation, with the highest level observed in IκB protein. After 5 hours of treatment the phosphorylation level started to decrease and to the end of assay continued to be similar to- or under the level of control untreated cells (Fig. 4). Compared to BOWES, phosphorylation signaling in A375 cells differed in later time points, as phosphorylation of JNK and p38, as well as of Akt/PKB continued to increase in ATO treated cells (Fig. S4). The patterns of phosphorylation signaling in NP realgar and ATO treated cells differed mainly between the cell lines, while were more similar within the respective cell line.

Effect of NP realgar on Nrf2 signaling. Metabolism of inorganic arsenic contributes to alteration of large number of transcription factors [28-31]. Among them Nrf2 plays a crucial role in the cellular protection against oxidative stress regulating the cellular antioxidant response. Therefore we have analyzed whether realgar modifies expression of Nrf2 mRNA and its downstream target HO-1 in melanoma cells. As is shown in Fig. 5 both mRNAs were upregulated in BOWES cell line, and HO-1 mRNA was increased in A375 cells (Fig. S5). Conversely, no concentration-dependent changes in the expression of Nrf2 mRNA in arsenic treated A375 cells were determined.

Autophagy plays a role in NP realgar toxicity. Inability of cells to reestablish cellular homeostasis after DNA damage or redox stress activates the processes leading to cell death. Recent studies suggest that the cytotoxic effect of arsenic is executed via apoptotic or autophagic cell death. The induction of autophagy is characterized by the elevation of LC3-II fragment, while the autophagic flux displays a decreased level of sequestosome, a 62 kDa multifunctional adaptor protein. Our results reveal that increased LC3-II level could be preferentially achieved at lower concentrations of both arsenic compounds indicating the activation of autophagy (Fig. 6A). The higher concentrations of both realgar and ATO led to the decrease of LC3-II expression associated with the fragmentation of PARP-1, a molecular marker of apoptosis. In BOWES cells cleavage of PARP-1 was accompanied by inhibition of autophagic flux, as p62 level inversely correlated with the autophagic activity (Fig. 6A). The different levels of LC3-II fragment in control untreated BOWES and A375 cells corresponded to the published results that melanoma cell lines can have high LC3-II basal protein level (Fig. S6A) [32].

Effect of CQ and Z-VAD-FMK on viability, mitochondrial potential, DNA cell cycle, and lysotracker staining. Autophagy flux can be blocked by administration of the lysosomotropic agent chloroquine (CQ), which inhibits the final step of autophagy, the fusion of autophagosomes with lysosomes. In the arsenic-treated BOWES cells the presence

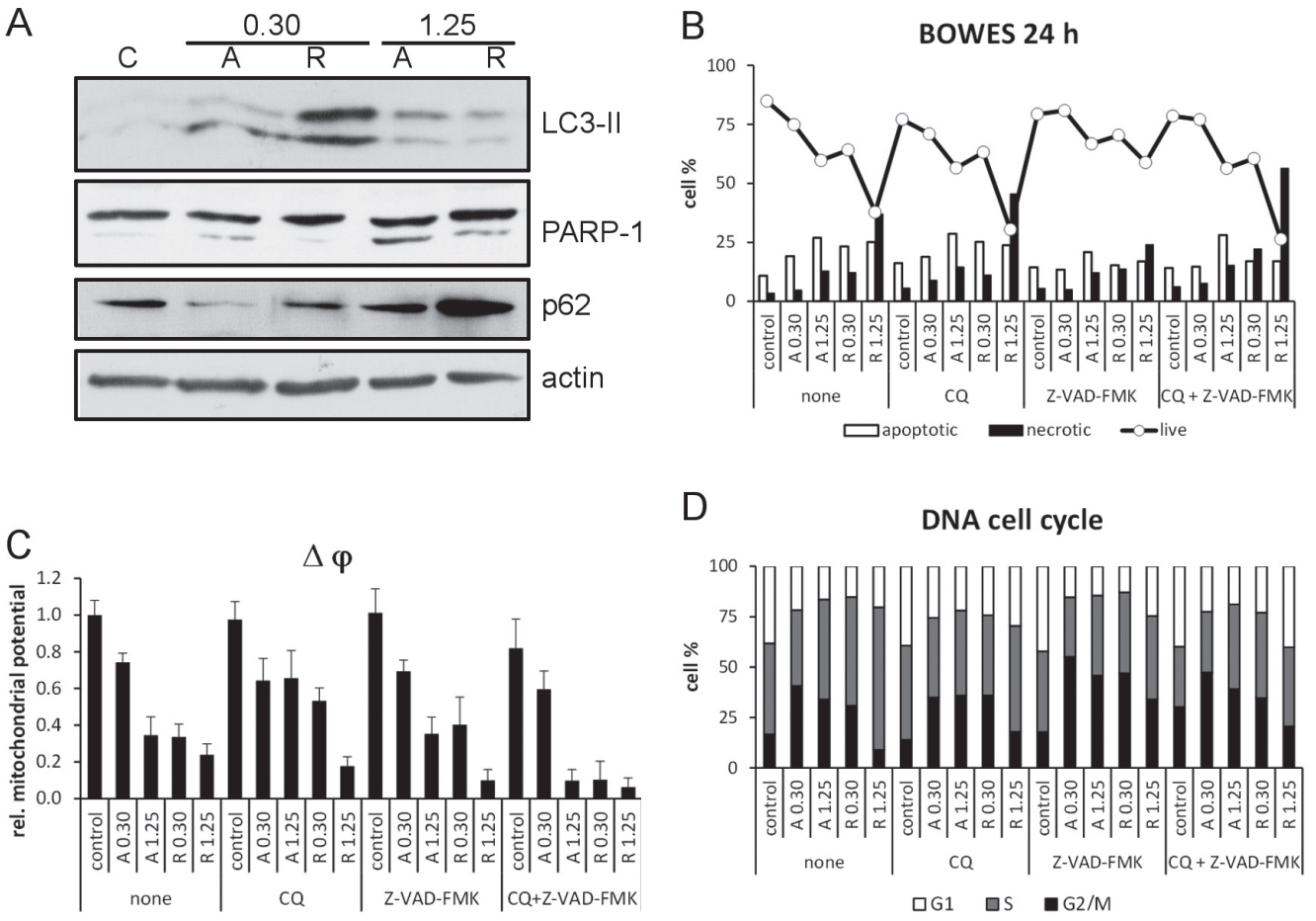

Figure 6. Effect of apoptosis and autophagy inhibition on viability (B), mitochondrial potential (C), cell cycle profile (D) of cells treated by NP realgar and ATO.

(A) BOWES cells were treated with 0.30 and 1.25 μg/ml As in the form of NP realgar (REA) and ATO for 24 hours and expression of LC3-II, PARP-1 and p62 was determined by western blotting. BOWES cells were treated with 10 μM CQ and 10 μM Z-VAD-FMK 1 hour prior to arsenic treatment with REA and ATO. Flow cytometric data acquisition by FACSCanto II and analyses of viability (B), mitochondrial membrane potential (C), and cell cycle (D) using FCS Express software were performed. Representative data at least of 2 experiments are presented.

of CQ caused a nonsignificant decrease of viability, whereas attenuated toxicity was observed in the presence of inhibitor of apoptosis Z-CAD-FMK (Fig. 6B, S6B). The pattern of cytotoxicity in the samples treated with both inhibitors was similar to the cytotoxic profile of the CQ alone. Furthermore, the analysis of the mitochondrial potential revealed the similar pattern of NP realgar and ATO effects in control and Z-VAD-FMK treated cells, whereas protective effect with CQ, or additive effects with both inhibitors in the samples were found with the exception of the samples with lower ATO concentration (Fig. 6C). Our results present two patterns of cell cycle G2/M phase accumulation in NP realgar and ATO treated cells; the first occurred in the presence and absence of CQ inhibitor, the second one refers to higher G2/M accumulation in the presence of a single Z-VAD-FMK or in its combination with CQ (Fig. 6D). The fusion of the autophagosomes with lysosomes, which represents the final stage of the autophagy, was then investigated by staining cells with Lysotracker-Red (LT), an acidic pH marker of lysosomes. First we have counted the number of LT spots per cell using the ImageStream analysis. Considering the fact that samples with high number of spots overlapped themselves, as demonstrated in the necrotic cell example (Fig. 7A) and precluded the counting, the measurement of LT fluorescence intensity was used for further analysis (Fig. 7B). In contrast to viability and mitochondrial potential patterns, where the efficiency of NP realgar overcame ATO, the LT staining pattern in BOWES cells was more similar to the pattern of the cell cycle changes in the sense of G2/M accumulation. Furthermore, the overall ATO treatment induced higher LT staining than realgar did in BOWES cells (the opposite was true for A375 cells) (Fig. S7) and the extent of changes in the presence of Z-VAD-FMK and in its combination with CQ was higher in comparison to the pattern of CQ effects and control cells that were not treated with inhibitors.

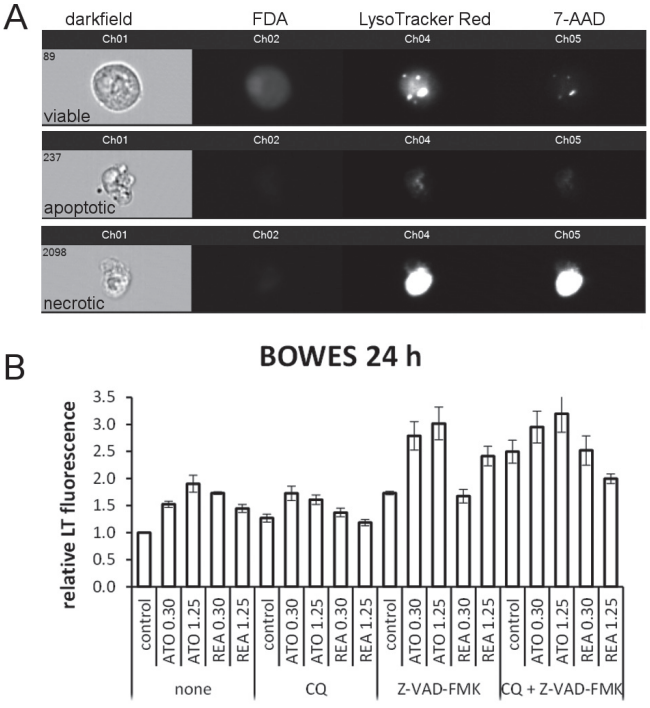

Figure 7. Effect of apoptosis and autophagy inhibition on lysosomal activity of BOWES cells treated by NP realgar and ATO.
(A) Representative pictures of viable, apoptotic, and necrotic cells analysis using ImageStream cytometer are shown. (B) BOWES cells were treated with 10 μM CQ and 10 μM Z-VAD-FMK 1 hour prior to treatement with 0.30 and 1.25 μg/ml As in the form of NP realgar (REA) and ATO for 24 hours.

Discussion

In the middle of nineties last century, two decades after Harbin report about clinical administration of ATO, the remarkable results of the Realgar-Indigo Naturalis Formula (RIF) application in APL (acute promyelocytic leukemia) patients were published as reviewed [33] Clinical data were followed by the molecular analysis of the mode of RIF action [34] and by the dissection of the synergistic effect of realgar and imatinib [35]. Recently, results of multicenter randomized controlled trial aimed at efficacy of oral RIF compared to intravenous ATO in induction and maintenance therapy for newly diagnosed APL were published [36]. The traditional Chinese medicine formulae often consist of numerous active ingredients and adjuvant components. Basically, realgar is a mineral with very low solubility in water and therefore leakage of arsenic from remedy is the question of bioavailability. It was shown that from some remedies like An Gong Niu Huang Wan release less arsenic than realgar while others like Liu Shen Wan show enhanced leaching of the arsenic [6].

In the present study we used realgar nanosuspension, which was prepared by milling in order to improve its solubility as reported previously our experiments and those of others [12, 14]. Our NP realgar IC_{50} data in melanoma cell lines are in line not only with recently published conclusion that nanosize scaled realgar particles have enhanced cytotoxicity [13], but also with observation that their IC_{50} values are even lower than IC_{50} values for ATO [11, 14]. Interestingly, the later study used chemical dissolution and microbial leaching process of realgar instead of milling. This may be important in the situation *in vivo*, since microorganisms, mainly sulfate reducing bacteria in gut environment, are also important contributors to the arsenic speciation change due to thiolation of methylarsenicals [37, 38]. Nowadays, many studies were aimed at assessment of the role of protein kinases in the cytotoxicity, cell death or differentiation induced by realgar. Inhibition of p38, JNK and ERK signaling pathway can synergize, enhance or suppress differentiation [39]. JNK was referred to be involved in U937 apoptosis induced by NP realgar [40], while activity of PI3K/AKT/mTOR signaling pathway was found to diminish apoptosis and preclude the eradication of leukemia stem cells by the realgar treatment [41]. Although the early peak of p38 activation is followed by a decrease of p38 phosphorylation in BOWES cells, the activity of p38 in A375 demonstrates the most visible change in the phosphorylation pattern induced by NP realgar.

Our phosphorylation experiments further revealed faint differences between NP realgar and ATO activation patterns within particular cell lines, while significant differences exist between the cell lines. In addition, we determined marked time-dependent changes in activities of the tested protein kinases and thus the knowledge of the relationship with other cellular processes might help to clarify the mechanisms of realgar action as demonstrated in the earlier study [42], which showed the time- and concentration-dependent changes in cellular glutathione, ROS level, mitochondrial potential, and p38 phosphorylation in realgar-treated HL60 cells. This myeloid leukemia cell line is often used as a model for terminal hematopoietic differentiation that could be started by realgar-induced increase of intracellular glutathione followed later by the decline to minimum at 6 h. Our study in BOWES and A375 cells revealed the increase of intracellular GSH level at 24 h of the treatment, possibly mediated by the upregulation of NRF2 mRNA as well as its downstream target HO-1, similarly to the reported increase of HO-1, Nrf2, and NFκB in endothelial cells treated by ATO [43]. These results also support the assumption that despite different physical forms of particulate and soluble arsenic, mechanisms of their action are very similar.

DNA damage, PARP cleavage and inhibition of glutathione reductase followed by caspase activation are the marks of cell response to ATO treatment [44]. Our analysis of the DNA damage through evaluation of γ-H2AX histone expression showed that NP realgar and ATO exhibit similar effects preferentially at higher concentration tested. In contrast, comparison of another pair of arsenic compounds – a therapeutic drug ATO, with a potent carcinogen sodium arsenite, revealed that ATO caused more severe damage in lung adenocarcinoma A549 cells than sodium arsenite [45]. The only difference, still

quantitative, that we have found between action of ATO and NP realgar, is in the course of autophagy; with the autophagic flux dominating at lower concentrations and the switch to apoptosis occurring at higher concentrations of both forms of arsenic. Moreover, NP realgar behaves as more proapoptotic arsenic form and the pan-caspase inhibitor more efficiently reduces NP realgar-induced cell death, despite the lack in protection against drop in the mitochondrial potential. Anyway, so far nobody has resolved a phenomenon, that equal amounts of arsenic in the form of NP realgar and soluble ATO have comparable cytotoxicity, despite the fact that only a part of arsenic atoms is accessible for chemical reaction in the nanoparticles of about 100 nm in diameter. One of possible explanation can be found in the article of T. Schwerdtle et al [46] about S(ulphur)-containing arsenic metabolites that modulated total cellular glutathione amount at picomolar concentrations. Recently it was shown that sodium arsenite treatment of normal cells induces prolonged activation of Nrf2 through autophagy dysfunction [29]. This observation corresponds to the fact found in certain human cancer types, where high sustained level of Nrf2 provides the resistance to treatment. In our study using melanoma cell lines only higher concentration of As (1.25 μg/ml) in NP realgar could induced the accumulation of p62.

We conclude that despite similar effects on cells of the same tissue origin, the actual involvement of signaling transduction and a capacity to maintain the cell homeostasis makes the difference in the fate of cells treated with different forms of arsenic. Our data also suggest that NP realgar is comparably or even more effective than ATO and that due to advantages of its nanoparticle formulation, it can potentially replace ATO in the therapeutic applications.

Acknowledgements: This study was supported by the research grants SAS-NSC JRP 2010/03 and VEGA 2/0177/11, VEGA 2/0027/14 from Slovak Academy of Sciences; project implementation TRANSMED 2, ITMS: 26240120030, supported by the Research & Development Operational Programme funded by the ERDF, APVV-0189-10 grant from Slovak R&D agency, and Cancer Research Foundation programs RFL2009 and RFL2012. Authors wish to express special thanks to Mrs. Margita (Pegy) Sulikova, for her excellent technical assistance.

References

[1] LEE TC, OSHIMURA M, BARRETT JC. Comparison of arsenic-induced cell transformation, cytotoxicity, mutation and cytogenetic effects in Syrian hamster embryo cells in culture. Carcinogenesis 1985; 6: 1421–1426. http://dx.doi.org/10.1093/carcin/6.10.1421

[2] TCHOUNWOU PB, PATLOLLA AK, CENTENO JA. Carcinogenic and systemic health effects associated with arsenic exposure--a critical review. Toxicol Pathol 2003; 31: 575–588.

[3] DODMANE PR, ARNOLD LL, KAKIUCHI-KIYOTA S, QIU F, LIU X et al. Cytotoxicity and gene expression changes induced by inorganic and organic trivalent arsenicals in human cells. Toxicology 2013; 312: 18–29. http://dx.doi.org/10.1016/j.tox.2013.07.008

[4] CALATAYUD M, DEVESA V, VELEZ D. Differential toxicity and gene expression in Caco-2 cells exposed to arsenic species. Toxicol Lett 2013; 218: 70–80. http://dx.doi.org/10.1016/j.toxlet.2013.01.013

[5] LU DP, QIU JY, JIANG B, WANG Q, LIU KY et al. Tetra-arsenic tetra-sulfide for the treatment of acute promyelocytic leukemia: a pilot report. Blood 2002; 99: 3136–3143. http://dx.doi.org/10.1182/blood.V99.9.3136

[6] WU XH, SUN DH, ZHUANG ZX, WANG XR, GONG HF et al. Analysis and leaching characteristics of mercury and arsenic in Chinese medicinal material. Analytica Chimica Acta 2002; 453: 311–323. http://dx.doi.org/10.1016/S0003-2670(01)01442-8

[7] KOCH I, SYLVESTER S, LAI VW, OWEN A, REIMER KJ et al. Bioaccessibility and excretion of arsenic in Niu Huang Jie Du Pian pills. Toxicol Appl Pharmacol 2007; 222: 357–364. http://dx.doi.org/10.1016/j.taap.2006.12.005

[8] XU W, WANG H, CHEN G, LI W, XIANG R et al. A metabolic profiling analysis of the acute toxicological effects of the realgar (As2S2) combined with other herbs in Niuhuang Jiedu Tablet using (1)H NMR spectroscopy. J Ethnopharmacol 2014; 153: 771–781. http://dx.doi.org/10.1016/j.jep.2014.03.050

[9] AN YL, NIE F, WANG ZY, ZHANG DS. Preparation and characterization of realgar nanoparticles and their inhibitory effect on rat glioma cells. Int J Nanomedicine 2011; 6: 3187–3194.

[10] CHEN P, YAN L, LENG F, NAN W, YUE X et al. Bioleaching of realgar by Acidithiobacillus ferrooxidans using ferrous iron and elemental sulfur as the sole and mixed energy sources. Bioresour Technol 2011; 102: 3260–3267. http://dx.doi.org/10.1016/j.biortech.2010.11.059

[11] WANG X, ZHANG X, XU Z, WANG Z, YUE X et al. Reversal effect of arsenic sensitivity in human leukemia cell line K562 and K562/ADM using realgar transforming solution. Biol Pharm Bull 2013; 36: 641–648. http://dx.doi.org/10.1248/bpb.b12-01015

[12] BALAZ P, FABIAN M, PASTOREK M, CHOLUJOVA D, SEDLAK J. Mechanochemical preparation and anticancer effect of realgar As4S4 nanoparticles. Materials Letters 2009; 63: 1542–1544. http://dx.doi.org/10.1016/j.matlet.2009.04.008

[13] TIAN Y, WANG X, XI R, PAN W, JIANG S et al. Enhanced antitumor activity of realgar mediated by milling it to nanosize. Int J Nanomedicine 2014; 9: 745–757.

[14] WU JZ AND HO PC. Evaluation of the in vitro activity and in vivo bioavailability of realgar nanoparticles prepared by cryo-grinding. Eur J Pharm Sci 2006; 29: 35–44. http://dx.doi.org/10.1016/j.ejps.2006.05.002

[15] KAMAT CD, GREEN DE, CURILLA S, WARNKE L, HAMILTON JW et al. Role of HIF signaling on tumorigenesis in response to chronic low-dose arsenic administration. Toxicol Sci 2005; 86: 248–257. http://dx.doi.org/10.1093/toxsci/kfi190

[16] MORALES AA, GUTMAN D, LEE KP, BOISE LH. BH3-only proteins Noxa, Bmf, and Bim are necessary for arsenic trioxide-

induced cell death in myeloma. Blood 2008; 111: 5152–5162. http://dx.doi.org/10.1182/blood-2007-10-116889

[17] GE F, LU XP, ZENG HL, HE QY, XIONG S et al. Proteomic and functional analyses reveal a dual molecular mechanism underlying arsenic-induced apoptosis in human multiple myeloma cells. J Proteome Res 2009; 8: 3006–3019. http://dx.doi.org/10.1021/pr9001004

[18] ANTOINE F, ENNACIRI J, GIRARD D. Syk is a novel target of arsenic trioxide (ATO) and is involved in the toxic effect of ATO in human neutrophils. Toxicol In Vitro 2010; 24: 936–941. http://dx.doi.org/10.1016/j.tiv.2009.11.011

[19] KUMAGAI Y AND SUMI D. Arsenic: signal transduction, transcription factor, and biotransformation involved in cellular response and toxicity. Annu Rev Pharmacol Toxicol 2007; 47: 243–262. http://dx.doi.org/10.1146/annurev.pharmtox.47.120505.105144

[20] ZHANG Y, WU JH, HAN F, HUANG JM, SHI SY et al. Arsenic trioxide induced apoptosis in retinoblastoma cells by abnormal expression of microRNA-376a. Neoplasma 2013; 60: 247–253. http://dx.doi.org/10.4149/neo_2013_033

[21] MARTINEZ VD, BUYS TP, ADONIS M, BENITEZ H, GALLEGOS I et al. Arsenic-related DNA copy-number alterations in lung squamous cell carcinomas. Br J Cancer 2010; 103: 1277–1283. http://dx.doi.org/10.1038/sj.bjc.6605879

[22] YANG TY, HSU LI, CHIU AW, PU YS, WANG SH et al. Comparison of genome-wide DNA methylation in urothelial carcinomas of patients with and without arsenic exposure. Environ Res 2014; 128: 57–63. http://dx.doi.org/10.1016/j.envres.2013.10.006

[23] ZHOU X, SUN H, ELLEN TP, CHEN H, COSTA M. Arsenite alters global histone H3 methylation. Carcinogenesis 2008; 29: 1831–1836. http://dx.doi.org/10.1093/carcin/bgn063

[24] WU JZ AND HO PC. Comparing the relative oxidative DNA damage caused by various arsenic species by quantifying urinary levels of 8-hydroxy-2‘-deoxyguanosine with isotope-dilution liquid chromatography/mass spectrometry. Pharm Res 2009; 26: 1525–1533. http://dx.doi.org/10.1007/s11095-009-9865-7

[25] BALAZ P, NGUYEN AV, FABIAN M, CHOLUJOVA D, PASTOREK M et al. Properties of arsenic sulphide As4S4 nanoparticles prepared by high-energy milling. Powder Tech 2011; 2011: 232–236. http://dx.doi.org/10.1016/j.powtec.2011.04.027

[26] WHO. Chapter 8 Chemical aspects. In. Guidelines for Drinking-water Quality 2011; fourth edition. ISBN 978 92 4 154815 1: 541.

[27] SHI H, SHI X, LIU KJ. Oxidative mechanism of arsenic toxicity and carcinogenesis. Mol Cell Biochem 2004; 255: 67–78. http://dx.doi.org/10.1023/B:MCBI.0000007262.26044.e8

[28] CHEN F AND SHI X. Intracellular signal transduction of cells in response to carcinogenic metals. Crit Rev Oncol Hematol 2002; 42: 105–121. http://dx.doi.org/10.1016/S1040-8428(01)00211-6

[29] LAU A, ZHENG Y, TAO S, WANG H, WHITMAN SA et al. Arsenic inhibits autophagic flux, activating the Nrf2-Keap1 pathway in a p62-dependent manner. Mol Cell Biol 2013; 33: 2436–2446. http://dx.doi.org/10.1128/MCB.01748-12

[30] WANG GZ, ZHANG W, FANG ZT, ZHANG W, YANG MJ et al. Arsenic trioxide: marked suppression of tumor metastasis potential by inhibiting the transcription factor Twist in vivo and in vitro. J Cancer Res Clin Oncol 2014; 140: 1125–1136. http://dx.doi.org/10.1007/s00432-014-1659-6

[31] MORZADEC C, MACOCH M, SPARFEL L, KERDINE-ROMER S, FARDEL O et al. Nrf2 expression and activity in human T lymphocytes: stimulation by T cell receptor activation and priming by inorganic arsenic and tert-butylhydroquinone. Free Radic Biol Med 2014; 71: 133–145. http://dx.doi.org/10.1016/j.freeradbiomed.2014.03.006

[32] XIE X, WHITE EP, MEHNERT JM. Coordinate autophagy and mTOR pathway inhibition enhances cell death in melanoma. PLoS One 2013; 8: e55096- http://dx.doi.org/10.1371/journal.pone.0055096

[33] CHEN SJ, ZHOU GB, ZHANG XW, MAO JH, DE TH et al. From an old remedy to a magic bullet: molecular mechanisms underlying the therapeutic effects of arsenic in fighting leukemia. Blood 2011; 117: 6425–6437. http://dx.doi.org/10.1182/blood-2010-11-283598

[34] WANG L, ZHOU GB, LIU P, SONG JH, LIANG Y et al. Dissection of mechanisms of Chinese medicinal formula Realgar-Indigo naturalis as an effective treatment for promyelocytic leukemia. Proc Natl Acad Sci U S A 2008; 105: 4826–4831. http://dx.doi.org/10.1073/pnas.0712365105

[35] ZHANG QY, MAO JH, LIU P, HUANG QH, LU J et al. A systems biology understanding of the synergistic effects of arsenic sulfide and Imatinib in BCR/ABL-associated leukemia. Proc Natl Acad Sci U S A 2009; 106: 3378–3383. http://dx.doi.org/10.1073/pnas.0813142106

[36] ZHU HH, WU DP, JIN J, LI JY, MA J et al. Oral tetra-arsenic tetra-sulfide formula versus intravenous arsenic trioxide as first-line treatment of acute promyelocytic leukemia: a multicenter randomized controlled trial. J Clin Oncol 2013; 31: 4215–4221. http://dx.doi.org/10.1200/JCO.2013.48.8312

[37] DC RUBIN SS, ALAVA P, ZEKKER I, DU LG, VAN DE WIELE T. Arsenic Thiolation and the Role of Sulfate-Reducing Bacteria from the Human Intestinal Tract. Environ Health Perspect 2014;

[38] ALAVA P, TACK F, LAING GD, DE WIELE TV. HPLC-ICP-MS method development to monitor arsenic speciation changes by human gut microbiota. Biomed Chromatogr 2012; 26: 524–533. http://dx.doi.org/10.1002/bmc.1700

[39] WANG N, WANG LW, GOU BD, ZHANG TL, WANG K. Realgar-induced differentiation is associated with MAPK pathways in HL-60 cells. Cell Biol Int 2008; 32: 1497–1505. http://dx.doi.org/10.1016/j.cellbi.2008.08.017

[40] WANG XB, GAO HY, HOU BL, HUANG J, XI RG et al. Nanoparticle realgar powders induce apoptosis in U937 cells through caspase MAPK and mitochondrial pathways. Arch Pharm Res 2007; 30: 653–658. http://dx.doi.org/10.1007/BF02977662

[41] HONG Z, XIAO M, YANG Y, HAN Z, CAO Y et al. Arsenic disulfide synergizes with the phosphoinositide 3-kinase inhibitor PI-103 to eradicate acute myeloid leukemia stem cells by inducing differentiation. Carcinogenesis 2011; 32: 1550–1558. http://dx.doi.org/10.1093/carcin/bgr176

[42] HU XM, YUAN B, TANAKA S, ZHOU Q, ONDA K et al. Involvement of oxidative stress associated with glutathione depletion and p38 mitogen-activated protein kinase activation in arsenic disulfide-induced differentiation in HL-60 cells. Leuk Lymphoma 2014; 55: 392–404. http://dx.doi.org/10.3109/10428194.2013.802779

[43] WANG L, KOU MC, WENG CY, HU LW, WANG YJ et al. Arsenic modulates heme oxygenase-1, interleukin-6, and vascular endothelial growth factor expression in endothelial cells: roles of ROS, NF-kappaB, and MAPK pathways. Arch Toxicol 2012; 86: 879–896. http://dx.doi.org/10.1007/s00204-012-0845-z

[44] RAY A, CHATTERJEE S, MUKHERJEE S, BHATTACHARYA S. Arsenic trioxide induced indirect and direct inhibition of glutathione reductase leads to apoptosis in rat hepatocytes. Biometals 2014; 27: 483–494. http://dx.doi.org/10.1007/s10534-014-9722-y

[45] JIANG X, CHEN C, ZHAO W, ZHANG Z. Sodium arsenite and arsenic trioxide differently affect the oxidative stress, genotoxicity and apoptosis in A549 cells: an implication for the paradoxical mechanism. Environ Toxicol Pharmacol 2013; 36: 891–902. http://dx.doi.org/10.1016/j.etap.2013.08.002

[46] LEFFERS L, UNTERBERG M, BARTEL M, HOPPE C, PIEPER I et al. In vitro toxicological characterisation of the S-containing arsenic metabolites thio-dimethylarsinic acid and dimethylarsinic glutathione. Toxicology 2013; 305: 109–119. http://dx.doi.org/10.1016/j.tox.2013.01.007

doi:10.4149/neo_2014_085

Supplementary Information

Realgar (As_4S_4) nanoparticles and arsenic trioxide (As_2O_3) induced autophagy and apoptosis in human melanoma cells in vitro

M. PASTOREK[1], P. GRONESOVA[1], D. CHOLUJOVA[1], L. HUNAKOVA[1], Z. BUJNAKOVA[2], P. BALAZ[2], J. DURAJ[1], T. CH. LEE[3], J. SEDLAK[1,*]

[1]*Cancer Research Institute, Slovak Academy of Sciences, Bratislava, 833 91, Slovakia;* [2]*Institute of Geotechnics, Slovak Academy of Sciences, Kosice, 043 53, Slovakia;* [3]*Institute of Biomedical Sciences, Academia Sinica, Taipei, 11529, Taiwan*

**Correspondence: jan.sedlak@savba.sk*

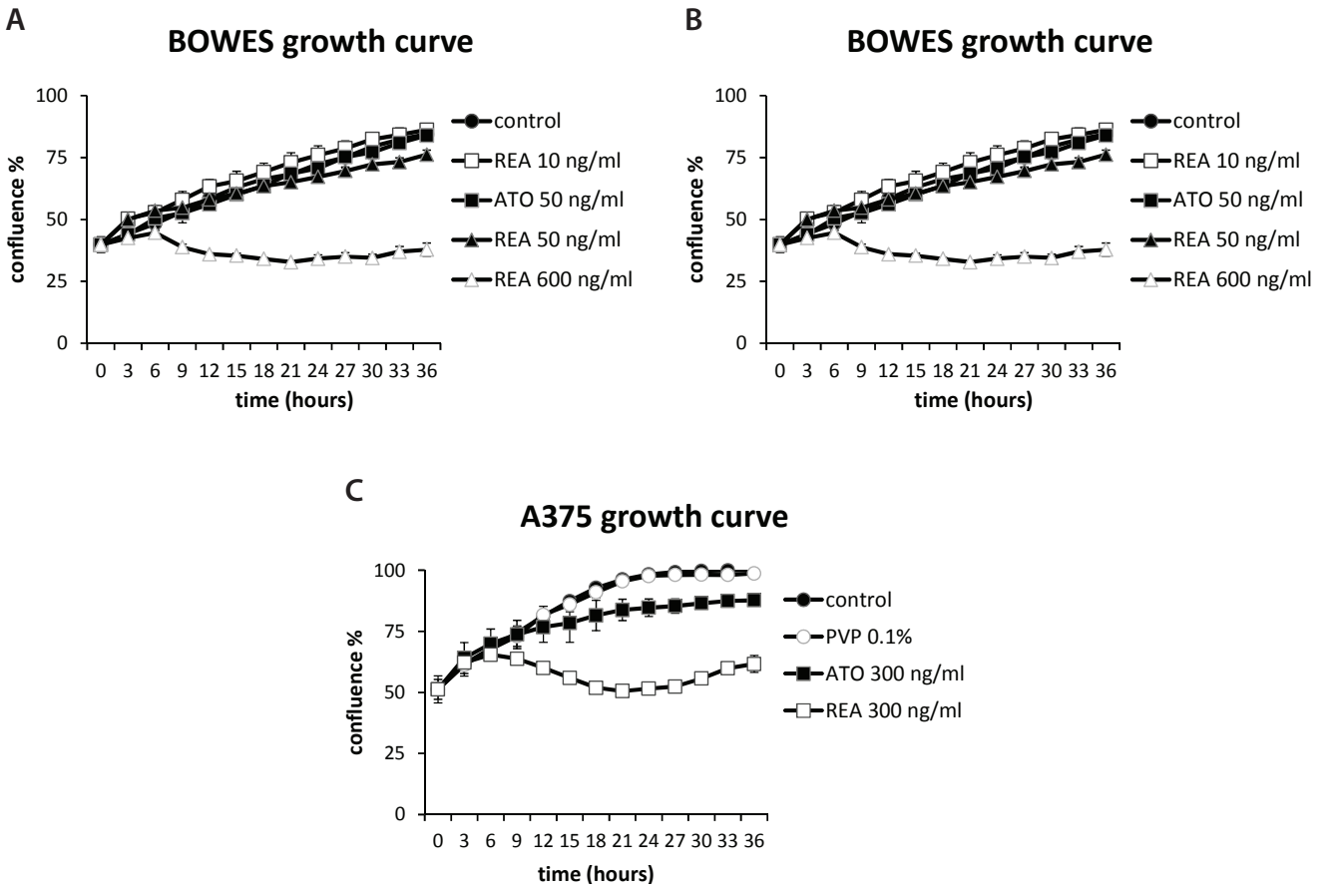

Figure S1. Effect of NP realgar and ATO treatment on BOWES and A375 cell proliferation.
BOWES (S1A) and A375 (S1B, S1C) cells were cultivated in the presence of NP realgar (REA) or ATO at the concentrations of As as indicated for 36 hours. The effect of 0.1% PVP (detergent used for milling of realgar) on proliferation of A375 cells is shown (S1C). Samples were done in quadruplicates and cell confluence was screened every 3 h using IncuCyte ZOOM microscope. The growth curves of cells treated with 300 ng/ml and 600 ng/ml As in the form of REA have bimodal distribution.

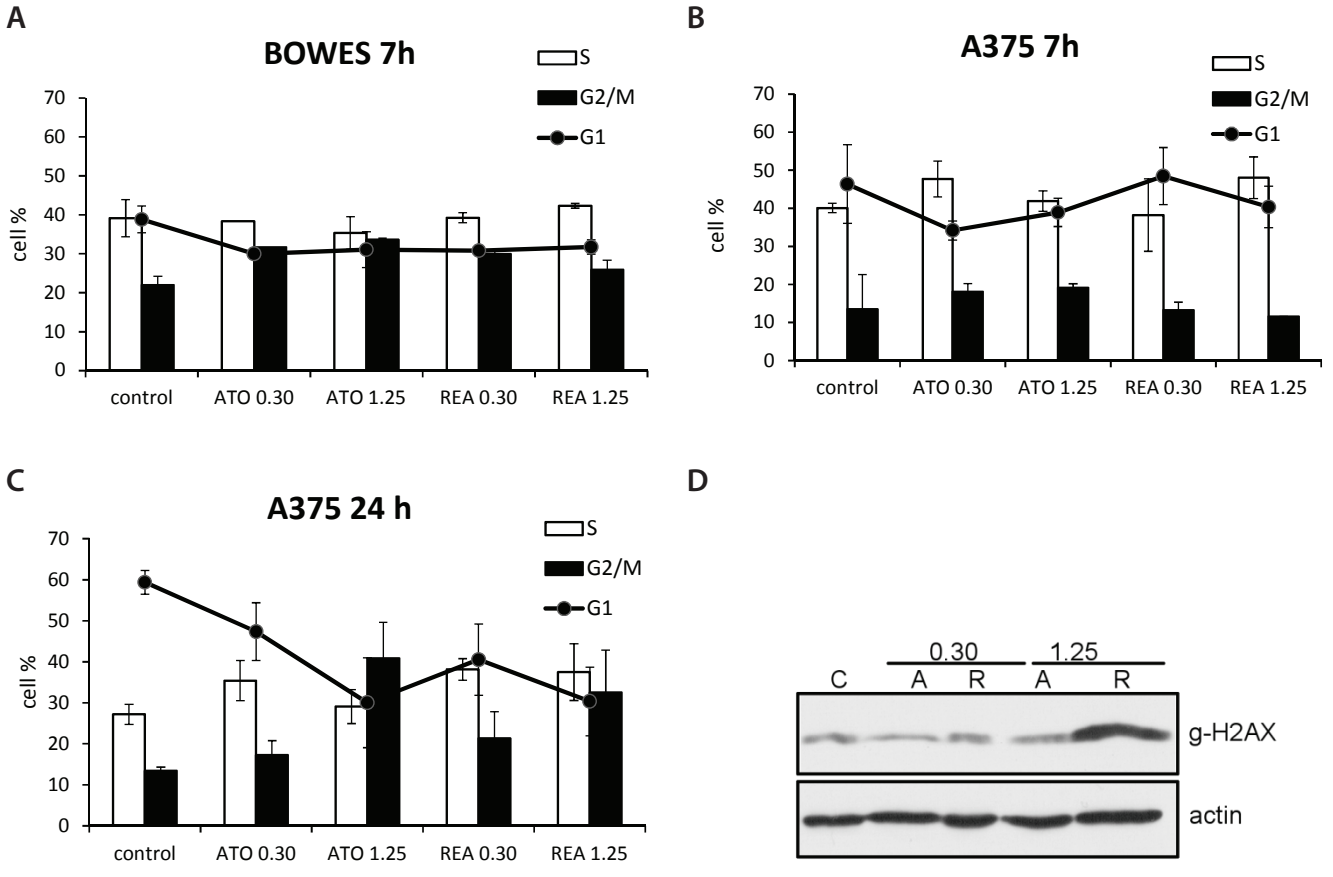

Figure S2. Cell cycle progression and DNA damage of BOWES and A375 cells treated with NP realgar and ATO.
BOWES (S2A) and A375 (S2B, S2C, S2D) cells were treated with NP realgar (REA) and ATO at the concentration 0.30 μg/ml and 1.25 μg/ml As for time indicated. DNA content was measured using FACS Canto II flow cytometer and analyzed by Multi-Cycle AV plug-in to FCS Express 3 software. The data of three independent experiments are presented as the mean +/- standard deviation. The representative western blott analysis of H2AX histone phosphorylation in A375 cells treated with REA and ATO for 24 hours is shown (S2D).

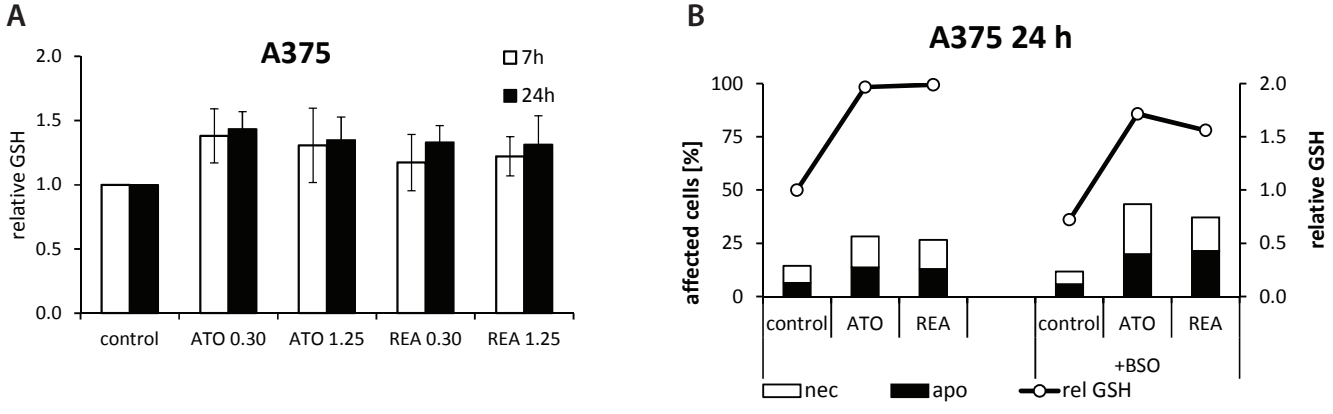

Figure S3. Changes of cellular GSH in A375 cells treated with NP realgar and ATO and their modulation by BSO.
A375 cells were treated with 0.30 μg/ml and 1.25 μg/ml As of NP realgar (REA) and ATO for 7 and 24 hours and GSH levels were measured by flow cytometry (S3A). A375 cells were treated without and with 50 μM BSO (S3B), an inhibitor of γ-glutamylcysteine syntethase required for GSH synthesis, 1 hour prior to treatement with 1.25 μg/ml As in the form of REA and ATO for 24 hours. The data of five (S3A) and three independent experiments are presented.

A375				
REA 1.25 µg/ml	1 h	3 h	5 h	7 h
Akt	1	1.20	2.68	1.67
ERK 1/2	1	1.38	1.40	1.71
IκB	1	1.91	1.39	1.46
JNK	1	1.84	2.84	2.67
p38	1	2.04	2.53	8.42
ATO 1.25 µg/ml	1 h	3 h	5 h	7 h
Akt	1	1.69	2.12	4.30
ERK 1/2	1	1.34	1.32	2.65
IκB	1	1.70	1.63	1.08
JNK	1	1.80	1.79	4.76
p38	1	1.96	2.55	14.59

Figure S4. Phosphosignaling modulation of Akt, ERK1/2, IκB, JNK and p38 kinases by NP realgar and ATO treatment in A375 cells.
A375 cells were treated with 1.25 µg/ml As of NP realgar (REA) and ATO for 1, 3, 5, and 7 hours and changes in relative phosphorylation were measured using Bio-Rad Bio-plex 200 machine. Data were normalized to the respective time-control value set to equal 1.0.

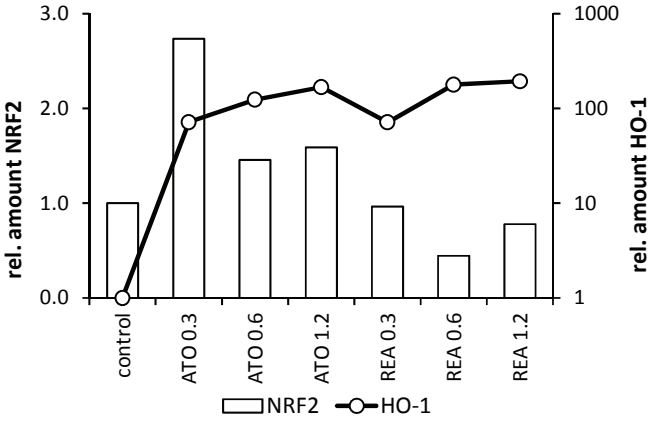

Figure S5. Quantitative PCR analysis of *NRF2* and *HO-1* expression after NP realgar and ATO treatment in A375 cells.
A375 cells were treated with increased concentration of As as indicated, in the form of NP realgar (REA) and ATO and expression of NRF2 and HO-1 mRNA was measured after 24 hours of treatment. The data of two independent experiments are presented.

A

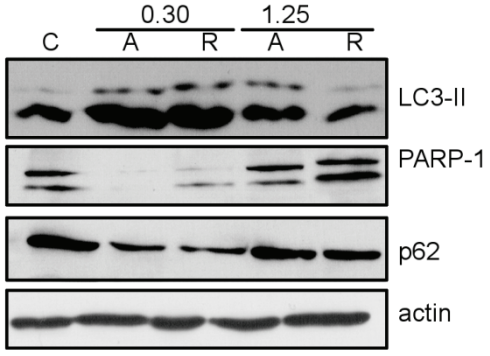

B

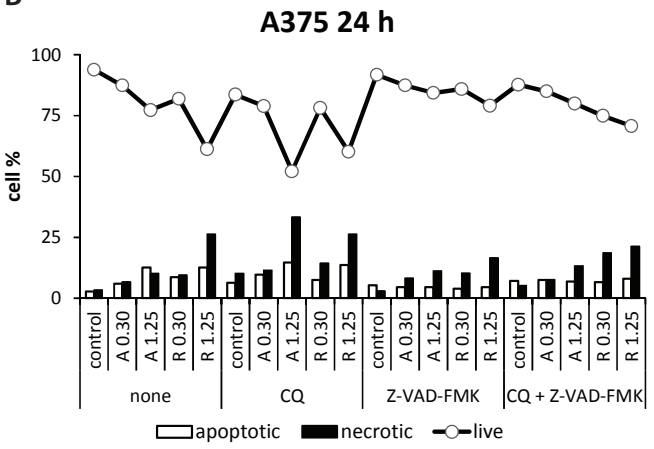

Figure S6A. Modulation of LC3-II, PARP-1 and p62 expression in A375 cells treated by NP realgar and ATO.
A375 cells were treated with 0.30 and 1.25 µg/ml As in the form of NP realgar (REA) and ATO for 24 hours and expression of LC3-II, PARP-1 and p62 was determined by western blotting. LC3-II expression, required for autophagosome formation, increased after treatment with 0.30 µg/ml As of REA and ATO and returned to control levels with concentration of 1.25 µg/ml As. PARP-1 cleavage and p62 expression decreased after treatment with 0.30 µg/ml As of REA and ATO and increased with concentration of 1.25 µg/ml As. The representative result of two independent experiments is shown.
Figure S6B. Effect of apoptosis and autophagy inhibition on viability of cells treated by NP realgar and ATO.
A375 cells were treated with 10 µM CQ, and 10 µM Z-VAD-FMK 1 hour prior to treatement with 0.30, and 1.25 µg/ml As in the form of NP realgar (REA) and ATO for 24 hours. The percentage of viable, apoptotic and necrotic cells was measured using FACSCanto II flow cytometer and data were analyzed by FCS Express 4 Flow software.

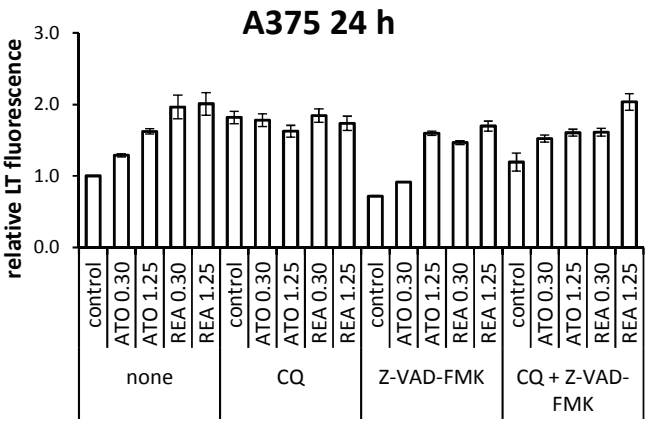

Figure S7. Effect of apoptosis and autophagy inhibition on lysosomal activity of cells treated by NP realgar and ATO.
A375 cells were treated with 10 μM CQ, inhibitor of autophagosome formation, and 10 μM Z-VAD-FMK, pan-caspase inhibitor of apoptosis, 1 hour prior to treatement with 0.30, and 1.25 μg/ml As in the form of NP realgar (REA) and ATO for 24 hours.